PCCP

Cite this: *Phys. Chem. Chem. Phys.*, 2012, **14**, 13010–13018

www.rsc.org/pccp

PAPER

Isoconfigurational molecular dynamics study of the kinetics of ice crystal growth†

Dmitri Rozmanov and Peter G. Kusalik*

Received 4th April 2012, Accepted 2nd August 2012
DOI: 10.1039/c2cp41073g

Spontaneous self-assembling, such as formation of molecular crystals, is a fascinating topic for investigation. Ability to initiate and control such transformations promises numerous benefits, but our knowledge of underlying mechanisms of such processes is rather limited. The process of freezing of water is an excellent testing ground for such studies. In this paper we report the results of a systematic molecular dynamics study of ice growth at three different temperatures below the melting point initiated from a number of initial interface structures within the isoconfigurational ensemble. It is shown that a specific structure at a growing ice–water interface is able to affect the growth process over a time scale of 1–2 ns. This structural effect can be characterized in terms of relative growth propensities. On the basis of the differences in the shape between isoconfigurational rate distributions and the rate distribution typical of the specific temperature several different kinds of relative growth propensities have been identified. The initial interfacial configurations employed in this work have been assigned using the proposed classification and possible mechanisms of propensity realization have been suggested for selected cases. Results reported in this paper clearly indicate that local structure effects can have significant impact on tendency for a particular ice surface to grow (or melt). The structural effect on ordering propensities is, most probably, a more universal behaviour and might be expected to be seen in other similar problems such as, for example, protein folding.

1 Introduction

Spontaneous self-assembling has always been a fascinating topic for investigation. Ability to initiate and control such transformations promises numerous benefits, but our knowledge of underlying mechanisms of such processes is rather limited. One of the more simple classes of self-assembling, or self-organization, is crystal formation, where an ordered crystal is created from a disordered and mobile liquid. Formation of molecular crystals is especially interesting because weak intermolecular interactions in them are the same or very similar to the interactions between amino-acids in the building blocks of large biological molecules in living organisms. These considerations make the process of freezing of water an excellent testing ground for investigating molecular self-organization. Due to fundamental technical difficulties with experimental probing of growing interfaces, the methods of numerical molecular simulations have become a *de facto* standard for these kinds of studies.

It is now accepted that heterogeneous crystal growth, such as formation of ice at the ice–water interface below the melting temperature, T_M, is a stochastic process.[1–4] This stochastic process is biased, and the bias comes from the degree of supercooling of the system.[3] This stochastic behaviour has been linked to the fundamental dynamic nature of the balance between local ordering and disordering governed by local fluctuations of thermodynamic properties.[1,3] However, it has been recently shown that ice growth rates demonstrate correlations at the time scale of approximately 1 ns.[4] It has been proposed that these correlations may stem from specific structural features present at the growing interface, and the specific time scale of 1 ns was suggested to be possible life time of those structural features.[4]

In a recent work by Widmer-Cooper *et al.*[5] a new molecular dynamics simulation technique was proposed, which allows us to study the importance of local structure for dynamics of the molecules in super cooled liquids. In this method a set of molecular dynamics simulations is initiated from multiple phase space points, in which the configurational part is the same for all the simulation, while the dynamic (kinetic) part varies between the simulations. The combined set of the resulting trajectories formed a so called *isoconfigurational ensemble*.[5] In practice the simulations are started from a single molecular configurations while the momenta of the particles are randomly sampled from the Maxwell–Boltzmann distribution corresponding to the desired temperature.[5] The isoconfigurational

Department of Chemistry, University of Calgary, 2500 University Drive NW, Calgary, Alberta T2N 1N4, Canada. E-mail: pkusalik@ucalgary.ca

† Electronic supplementary information (ESI) available. See DOI: 10.1039/c2cp41073g

ensemble average displacement of a particle (displacement of the same particle averaged over all the trajectories) demonstrates dynamics independent *propensity for motion* of this particle, which comes from the common initial structure. Later, the method has been successfully applied in a number of other studies.[6,7]

In this work we apply this powerful technique of molecular dynamics simulations in an isoconfigurational ensemble[5,6] to gain knowledge on importance of specific ice–water interface structures on crystal growth of the basal (0001) face of hexagonal ice I_h, as well as to evaluate time scales of potential correlations in growth kinetics associated with these structures. Such information would extend our understanding of the processes of heterogeneous crystallization, as well as provide insight into mechanisms of the general class of processes of self-organization. In this paper we report the results of a systematic molecular dynamics study of ice growth at three different temperatures below the melting point initiated from a number of specific initial interface structures in an isoconfigurational ensemble.[5,6] It has been suggested previously in ref. 4 that growth rates from many short independent simulations under the same conditions can be averaged to produce an accurate average growth rate; testing this approach to measuring growth rates was also a goal of this work. The rest of the paper is organized as follows. The following Section 2 details simulations performed and the methods used in this work. The computational details are given in Section 3. The results of performed simulations along with appropriate discussion will be given in Section 4. Finally, our conclusions will be summarized in Section 5.

2 Methods and simulations

Three independent systems of 3264 molecules of water (S1–S3) were used to evaluate structural dependence of the crystal growth rates of the basal face of hexagonal ice I_h at three different supercoolings relative to the melting temperature: $T_M - 24$, $T_M - 12$, and $T_M - 3$ K. The intermolecular potential of water molecules was represented by the TIP4P-2005 model of water.[8] This model has the the melting temperature of 251 K,[3,8,9] based on which, the absolute temperature values for simulations were 227, 239, and 248 K, respectively.

The three initial systems, S1–S3, were prepared by generating a crystal lattice of oxygen atoms in the simulation box using crystallographic parameters[10] of hexagonal ice I_h so that the basal (0001) face was in the XY plane. Hydrogen atoms were then randomly assigned using the ice rules.[10,11] Consequently, the total dipole moment of the ice in the simulation box was minimized by flipping the orientation of a random water molecule. The orientations of neighboring molecules were also readjusted to satisfy the ice rules. These crystals of ice were equilibrated for 50 ps at 250 K and 1 bar, the melting point of the model, under temperature and pressure control. To generate two phase systems the translational motion of water molecules of the intended ice phase was artificially frozen while the systems were heated to 500 K under constant volume conditions. After melting, the system was equilibrated at 250 K and 1 bar for another 100 ps. The three independent systems were prepared from the same ice crystal by varying the Z-position of the ice slab in the simulation box by 3.6 Å (1 ice layer). The systems had approximate dimensions of 27 × 31 × 121 Å, and contained approximately equal amounts of ice and water. The separation between ice–water (interface A) and water–ice (interface B) interfaces was approximately 60 Å, which is sufficient to consider the interfaces to be independent.[1] Then each of the systems was equilibrated at the three temperatures for 2 ns under pressure and temperature control to produce three independent systems at each of the temperatures. The equilibration time for the initial system was taken longer than the estimated correlation time of ice growth at the lowest temperature[4] to ensure independence of the initial structures.

The isoconfigurational simulations[5] were carried out as follows. For each initial system the molecular positions were kept unchanged and the molecular momenta were randomly redistributed between the molecules to produce 200 different initial phase points of the same structure and energy (probability). Randomization of momenta produced a slight net translational motion of the center of mass (COM) of the system as well as a slight rotation of the entire system around it, which were removed. The removed kinetic energy of the COM motion was returned to the system by appropriate rescaling of the corrected molecular linear momenta. All 200 phase points were then propagated for 4 ns under temperature and pressure control. The conducted simulations produced 200 trajectories, 4 ns each, at 3 independent initial configurations and at 3 different temperatures. As each system had 2 growing interfaces, all together, these 1800 simulations resulted in 14.4 μs of ice growth data. The positions of both A and B interfaces were found according to the interface detection method described in ref. 3. The detection was done using 256-bin density profiles along the Z-dimension of the simulation box sampled over 10 ps; 8-bin subsets of the density profile were used to evaluate local molecular layering. Ice growth rates were determined by relating the change in the position of a specific interface to the time separation between measurements (time window); 1 and 2 ns time windows were used for rate determination in this work.

The following discussion deals with a number of different growth rate estimates, so in order to avoid confusion a special notation to describe growth rates is introduced: $R_{t_0,i}^{(\Delta t)}$ identifies a growth rate in a system i estimated using a time window Δt starting from the simulation time t_0. To indicate the average of N such rates the notation ${}^{N}\bar{R}_{t_0}^{(\Delta t)}$ will be used.

We have shown earlier[3] that there is a size effect in crystal growth studies related to the reduction of the entropy of the liquid phase under periodic boundary conditions. That work demonstrated that a system of 2880 water molecules was close to the point of saturation of this effect. In this work we used systems of 3264 molecules and expect the effect to be negligible. At the same time there is reason to keep the size of the system small enough so that the specifics of local space–time fluctuations affecting local growth behaviour are not lost. Hence, if the interface surface is too large there will be many topological features at the interface so that properties specific to these features will be averaged out, including any potential effect on the growth rate.

3 Simulation details

The simulations were performed under periodic boundary conditions. The short-ranged Lennard-Jones interactions were cut off at 10.0 Å which corresponds to relative error in forces of less than 10^{-4}. The electrostatic interactions were evaluated by the smooth particle mesh method of Ewald summation (SPME).[12] The SPME parameters were chosen so that the relative force error was similar to that of the Lennard-Jones interactions. Specifically, the real space cut off was 8.0 Å, the Ewald splitting parameter $\alpha = 0.424$, the spacing for charge density grid was 0.75–0.79 Å, depending on the direction, and 8th order splines were used for interpolation. The translational molecular motion was integrated using the velocity Verlet method,[13] while for the rotational motion an iterative quaternion based rotational velocity Verlet algorithm[14] was used with convergence tolerance of 10^{-10}. The time step for numerical integration of equations of motion was 2 fs. The temperature control was provided by separate Nosé–Hoover 4-element chain thermostats[15,16] for each molecule (1 chain per 6 degrees of freedom) with all four time constants equal to 1.0 ps. The pressure was maintained at 1 bar by using an anisotropic Berendsen type barostat[17] with the time constants of 100, 100, and 5 ps for X, Y, and Z directions, respectively. The value of the compressibility β was that of liquid water, 4.5×10^{-5} bar^{-1}. The simulations were performed using our own in-house molecular dynamics code.

4 Results and discussion

4.1 Average rates

The ice growth rates within one set of 200 isoconfigurational runs are expected to correlate if the initial structure affects the growth process. Based on the finding reported in ref. 4 the time scale for the correlation is expected to be of the order of 1 ns. To test this hypothesis the ice growth rates were evaluated using the first and the last 2 ns of 4 ns simulation trajectories producing 6 isoconfigurational sets of rates at each temperature for each of the segment, or, using the notation explained in Section 2, $\{R^{(2)}_{0,i}\}_{\mathrm{SIT}}$ and $\{R^{(2)}_{2,i}\}_{\mathrm{SIT}}$, where SIT stands for system-interface-temperature and identifies a specific set of isoconfigurational simulations. The average growth rates were calculated for these two parts of the trajectories for each interface and for each isoconfigurational set, generating isoconfigurational ensemble average rates, or SIT-rates, ${}^{200}\bar{R}^{(2)}_{0,\mathrm{SIT}}$ and ${}^{200}\bar{R}^{(2)}_{0,\mathrm{SIT}}$. The average rates at a specific temperature or T-rates (averaged over all systems and interfaces), ${}^{1200}\bar{R}^{(2)}_{0,T}$ and ${}^{1200}\bar{R}^{(2)}_{0,T}$, were also calculated for both the time segments. Table 1 shows all the SIT-rates and Table 2 demonstrates the T-rates.

Using 2 ns segments ensured that the second part of the growth data will not correlate with the first part (expected correlation time is $\approx$1 ns[4]), or in other words, that the configurations will diverge from the single initial configurational point to a set of random uncorrelated configurations consistent with the specific temperature. Hence, the statistics of the SIT-rates found from the first, initial, part should be biased by the structural correlations, while the second, last, part should demonstrate the unbiased growth behaviour typical for this temperature.

Table 1 Isoconfigurational SIT growth rates found from the first, ${}^{200}\bar{R}^{(2)}_0$, and the last, ${}^{200}\bar{R}^{(2)}_2$, 2 ns of simulations averaged over 200 isoconfigurational runs. The corresponding standard deviations (${}^{200}\sigma^{(2)}_0$ and ${}^{200}\sigma^{(2)}_2$), of isoconfigurational rates are also shown. Note that configurations with the same labeling at different temperatures are different

T (K)	System	Interface	${}^{200}\bar{R}^{(2)}_0$ (Å ns^{-1})	${}^{200}\bar{R}^{(2)}_2$ (Å ns^{-1})	${}^{200}\sigma^{(2)}_0$ (Å ns^{-1})	${}^{200}\sigma^{(2)}_2$ (Å ns^{-1})
227	S1	A	1.31	0.57	0.94	1.05
		B	−0.02	0.42	0.82	0.93
	S2	A	0.15	0.51	1.20	0.95
		B	0.01	0.46	0.67	0.91
	S3	A	0.61	0.41	1.26	1.12
		B	0.23	0.37	0.57	0.85
239	S1	A	0.79	0.62	0.83	0.92
		B	0.72	0.71	0.84	0.87
	S2	A	1.67	0.79	0.80	0.93
		B	0.50	0.77	0.84	1.00
	S3	A	1.05	0.70	0.84	0.95
		B	0.78	0.68	0.83	0.97
248	S1	A	0.08	0.23	1.01	0.85
		B	0.27	0.18	0.77	0.80
	S2	A	0.18	0.17	0.79	0.75
		B	0.31	0.18	0.68	0.88
	S3	A	0.05	0.14	0.67	0.79
		B	−0.17	0.14	0.91	0.78

Table 2 Average growth rates for the three temperatures found from the first (${}^{1200}\bar{R}^{(2)}_0$) and the last (${}^{1200}\bar{R}^{(2)}_2$) 2 ns of simulations averaged over all 1200 rates at the same temperature. The corresponding standard deviations in the set of 1200 rates (${}^{1200}\sigma^{(2)}_0$ and ${}^{1200}\sigma^{(2)}_2$), as well as the standard deviations of the six average SIT rates from Table 1 (σ_{R_0} and σ_{R_2}) are also shown

T (K)	${}^{1200}\bar{R}^{(2)}_0$ (Å ns^{-1})	${}^{1200}\bar{R}^{(2)}_2$ (Å ns^{-1})	${}^{1200}\sigma^{(2)}_0$ (Å ns^{-1})	${}^{1200}\sigma^{(2)}_2$ (Å ns^{-1})	σ_{R_0} (Å ns^{-1})	σ_{R_2} (Å ns^{-1})
227	0.38	0.46	1.07	0.97	0.51	0.07
239	0.92	0.71	0.92	0.94	0.41	0.06
248	0.12	0.18	0.83	0.81	0.18	0.03

One can see in Table 1 that the ${}^{200}\bar{R}^{(2)}_2$ rates are quite similar while the variation between ${}^{200}\bar{R}^{(2)}_0$ SIT-rates at the same temperature is much wider. For example, at $T = 239$, ${}^{200}\bar{R}^{(2)}_0$ values span the range of 0.50–1.67 Å ns^{-1} while the ${}^{200}\bar{R}^{(2)}_2$ values are within the range of 0.62–0.79 Å ns^{-1}. In contrast, the standard deviations, ${}^{200}\sigma^{(2)}_0$ and ${}^{200}\sigma^{(2)}_2$, show similar variations of the growth rates in different isoconfigurational sets for both the initial and final parts of the simulations.

The T-rates for both 2 ns segments, ${}^{1200}\bar{R}^{(2)}_0$ and ${}^{1200}\bar{R}^{(2)}_2$ shown in Table 2, are similar, as well as the standard deviations of rates within these combined sets. The standard deviations of the six SIT-rates, σ_{R_0} and σ_{R_2}, however, differ very substantially between the segments. In the first 2 ns, the SIT-rates are strongly affected by the initial structure at the interface and differ significantly between different configurations. In the last 2 ns, the SIT-rates become essentially the same because of diverging configurations, so that 200 trajectories of each initially isoconfigurational SIT-simulation sample a similar configurational space particular to that temperature. Thus, the statistical analysis of the SIT-rates and T-rates demonstrates that specific structures at growing interfaces indeed influence the process of ice growth.

Assuming that configurations in one isoconfigurational set of simulations become completely independent after 2 ns, the

T-rate, ${}^{1200}\bar{R}^{(2)}_{2,T}$, is expected to be equivalent to a rate found from a single 2.4 μs long simulation.[4] These rates (Table 2) agree very well with previously reported rate values of 0.45 ± 0.12, 0.61 ± 0.14, and 0.17 ± 0.14 Å ns^{-1} at the same temperatures of 227, 239, and 248 K, respectively.[4] The uncertainties of ${}^{1200}\bar{R}^{(2)}_{2,T}$ values taken as 95% confidence interval for an average of 1200 normally distributed samples are ±0.06, ±0.06, and ±0.05 at 227, 239, and 248 K, respectively. Hence, these are the most precise rate estimates for the ice growth of any water model to date. The rates in ref. 4 were found by averaging results from three 80 ns steady state molecular dynamics simulations. The rates in this work were found from many 4 ns simulations instead and are very amenable to coarse grain parallelism. Such simplification is clearly an improvement of the method.

4.2 Time relaxation of SIT-rates

To investigate time correlations of the growth rates within isoconfigurational sets the time evolution of the growth rates was obtained using 1 ns moving time windows. These time evolutions of the SIT-rates as well as the average T-rate at each of the three temperatures are shown in Fig. 1. The time evolution of corresponding standard deviations of the six SIT-rates is shown in Fig. 2. One can see the obvious effect of the initial structure, rates from different configurations on average behave differently. Some of the SIT configurations demonstrate strong propensities to grow faster or slower (or even melt) relative to the typical growth rate at a specific temperature. For example, at 227 K (see Fig. 1(A)) the system is deeply supercooled and yet, the interface S2B tends to melt quickly, while the interface S1A shows propensity to grow much faster than expected from the average behaviour at such low temperature. Interestingly, the average T-rates are similar at the beginning and at the end of the simulations, that is, while each of the interfaces shows its own growth pattern, all six of them provide adequate sampling of the "natural" configurational space of the ice–water interface and produce correct average behaviour.

The time required for the SIT-rates to converge to the typical growth rate at the specific temperature can be considered as the correlation time and should relate to the life time of the structural features at the the surface of an interface. The plots of the standard deviations of SIT-rates in Fig. 2 provide a clear picture. At the lowest temperature, it takes almost 2 ns for all SIT-rates to become independent of initial configuration (see Fig. 2(A)), at 239 K (Fig. 2(B)) the correlation disappears after ≈0.5 ns. The correlation at the temperature just below the melting point, 248 K, is more complex (Fig. 2(C)): most of the correlation disappears quickly, within 0.3 ns, but then variation between SIT-rates remains somewhat elevated for another 1.4 ns. Unexpectedly, the correlation time at 248 K seems to be longer than that at 239 K. Careful examination of Fig. 1 shows that at 227 K the individual SIT-rates gradually and monotonically relax to the "natural" value; at 239 K this relaxation is also gradual and monotonous but quicker; at 248 K the initial relaxation is fast and often overshoots the "natural" growth rate, then it takes longer time to relax that "overshot" behaviour back to the average at this temperature value. Another way to see this structural effect is to consider

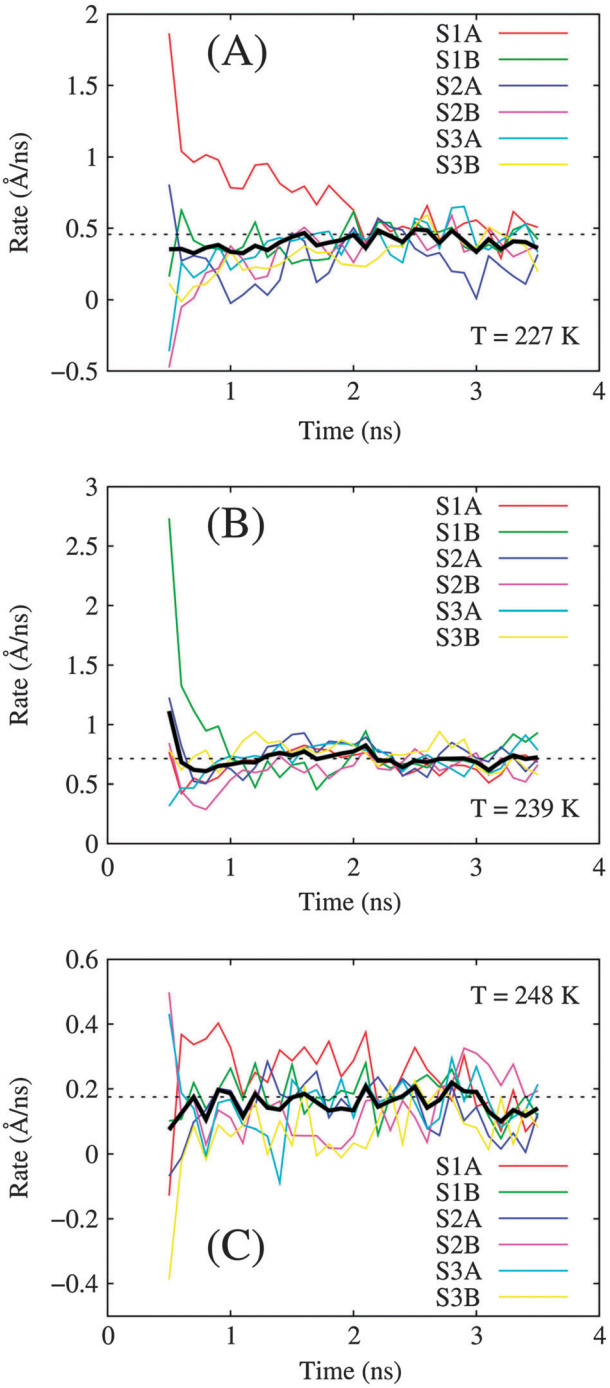

Fig. 1 The six isoconfigurational SIT-rates, ${}^{200}\bar{R}^{(1)}_{t}$, at the three temperatures, 227 K, (A), 239 K, (B), and 248 K, (C). The rate curves are obtained as growth rates for 1 ns moving time window every 100 ps; the points (values) correspond to the mid-point for the window. In all the cases, the thick black line indicates the T-rate, ${}^{1200}\bar{R}^{(1)}_{t}$, averaged over all 6 SIT-rates. The horizontal dashed line shows the estimated growth rate at this temperature taken as ${}^{1200}\bar{R}^{(2)}_{2}$ value from Table 2.

that the growth rate is low at 248 K due to proximity to the melting point, so, if a specific configuration shows a strong propensity to growth or to melt, then it must realize its propensity to form a structure of the opposite propensity to compensate for "unusual" fluctuation. This effect can be seen

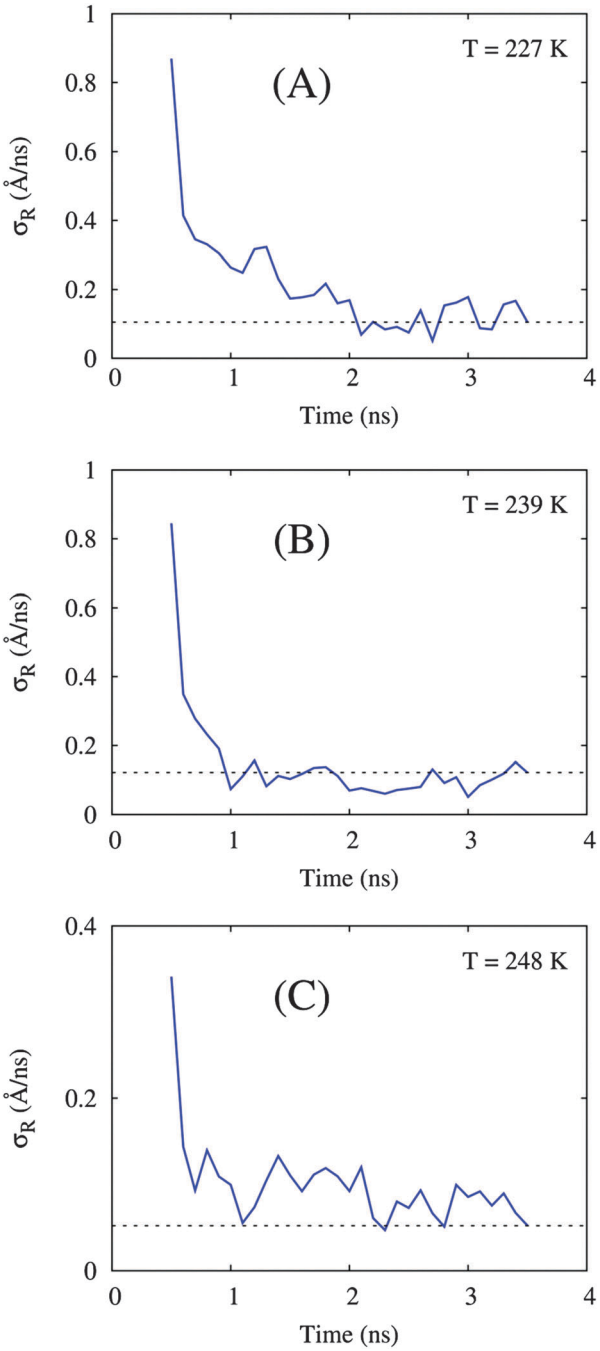

Fig. 2 The time evolution of the standard deviations, σ_R, of the six isoconfigurational SIT growth rates (shown in Fig. 1) at the three temperatures, 227 K, (A), 239 K, (B), and 248 K, (C). In all the cases, the dashed line indicates the typical standard deviation for rates averaged over 200 1 ns rates taken as the last value of the curve.

in S1A, S2B, and S3A isoconfigurational runs in Fig. 1(C). While the effect is relatively weak the small absolute value of the growth rate at 248 K makes it more noticeable. At lower temperatures the relaxation apparently occurs slower so that the correlation disappears without going into such "compensation" mode.

In ref. 4 it has been shown that the growth rate correlations at different temperatures are limited by so called break-point times, τ_B, which were estimated to be 2.14, 1.70, and 1.77 ns at 227, 239, and 248, respectively (see Table 4 in ref. 4). Now, it is reasonable to assume that those break-point times and the SIT-rate relaxation times determined in this work are directly related.

4.3 Growth rate probability distributions

To obtain better insight into the nature of the observed structural growth propensities the distribution of growth rates from individual SIT-simulations could be compared with the rate distribution typical for a specific temperature. Fig. 3 shows the total distributions of all 1200 individual growth rates from 1 ns time windows at the beginning and at the end of the simulations at the three temperatures. The rate distributions at the end of the simulations should represent the typical distributions at these temperatures. Apparently, the total distributions at the beginning of the simulations are very similar to the typical distributions of growth rates, meaning that, while each of six initial SIT-configurations has its own growth propensity, their average represents the typical behaviour well, *i.e.* six configurational points are essentially enough to sample the full configurational space at a specific temperature.

The shape of the distributions in Fig. 3 reveals interesting details about the crystal growth mechanism: at all the three temperatures, the distributions appear to be composed by three overlapping peaks. The strongest, central, peak has its maximum positioned at zero, which means that in most simulations the position of the interface did not actually change during 1 ns of observation. Two other peaks are positioned symmetrically around the central peak, at about ± 3.6 Å ns^{-1}. These side peaks correspond to "single-layer" interface velocities: during the time of observation (1 ns) in those simulations the interface has grown or melted by one layer of ice (the distance between ice layers in the Z-direction is ≈ 3.6 Å). The relative magnitudes of these peaks determine the actual growth rate at a specific temperature. These distributions are consistent with the discrete, layer-by-layer, mechanism of growth of the basal face of hexagonal ice I_h proposed earlier.[4,18,19]

The probability distributions of rates from individual isoconfigurational sets, shown in Fig. 4, demonstrate striking configurational dependence. The rate distributions for the initial 1 ns can differ from the typical shape substantially, apparently biased by the relative growth propensity of its initial interface structure, while the distribution for the last 1 ns becomes similar to the distribution characteristic for this temperature. Based on the shape of the probability distribution of initial growth rates and its mean value the following seven types of relative growth propensities were identified: a specific interface growth faster than the average (notation "+"); slower ("−"); similar ("0"); similar to the average, but the distribution is more narrow ("0*"), and the mean value is similar to that of the average distribution, but the distribution is essentially bimodal ("+−"); finally, "+*" and "−*" propensities demonstrate significantly faster or slower growth, respectively. The configurations used in this work were classified following these notations as shown in Table 3. Numerical values of the mean distribution, standard

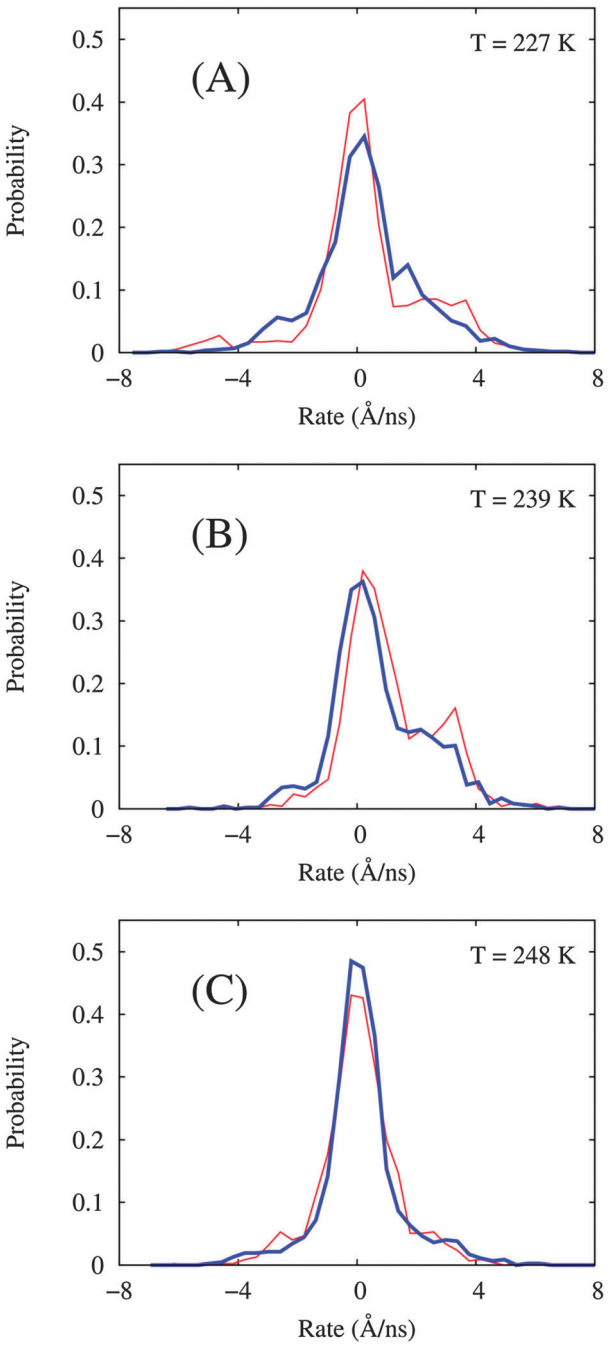

Fig. 3 The combined probability distributions of 1200 ice growth rates found using 1 ns time windows at the beginning (thin lines) and at the end (thick lines) of the simulation for the three different temperatures, 227 K, (A), 239 K, (B), and 248 K, (C).

deviation, skewness, and kurtosis for all isoconfigurational rate sets as well as for the total rate set at each temperature are given in Tables S1 and S2 in ESI.†[20]

The assigned propensities for specific configurations are also shown in Fig. 4. Fig. 4(A) shows an example of melting propensity of a configuration which is, probably, "between layers": the peak's maximum is positioned below zero, totally atypical, but not at the "single-layer" velocity of -3.6 Å ns^{-1}. This is an indication that in most of the simulations some ice melted but less than a full layer, the only reasonable explanation under conditions of a layer-by-layer mechanism is that the simulations start from a partially melted layer. Fig. 4(B) demonstrates a very strong propensity to form a new layer of ice. Interestingly, the main peak corresponds to the "single-layer" velocity, which means that most of the simulations have grown a new layer of ice, which did not exist initially, so that, it has to be the configuration of the liquid side of the interface which is responsible for this fast growth. The growth propensity shown in Fig. 4(C) results in a growth rate similar to that of the typical one, but the interface is more stable, as its position did not change in most of the simulations. The expected growth rate at this temperature is similarly low, but the typical dynamic balance between growth and melting is substantially more important (some growth and melting are expected but not present in this specific case). Finally, Fig. 4(D) gives an example of a very unstable interface with similar propensities to melt and grow at the same time. This behaviour is clearly not typical at this temperature. The melting velocity corresponds to the "single-layer" one, while the growth velocity is peaked at approximately one half of it, which means that this configuration prefers to either melt one full layer of ice or, equally likely, to form a new structural feature on the surface which shifts the detected interface position by approximately a half-layer, such as a microfacet.[21,22] This is an interesting behaviour, which is difficult to explain, we can speculate that in this case the outer layer of ice could be somewhat disordered and unstable while the liquid side of the interface is already partially ordered, similarly to the case shown in Fig. 4(B), or there may be a precursor of a potential microfacet on the surface. Hence, if the melting propensity is realized the ordering of the liquid phase or the structured surface feature cannot stop it and the top layer of ice melts completely. However, if the ice layer survives and the growth propensity plays its part, then the microfacet on the surface is fully formed with high probability. The distribution plots for the other isoconfigurational simulations performed in this work corresponding to the relative growth propensities from Table 3 can be found in Fig. S1–S3, ESI† for this paper.[20]

4.3.1 Interface surface topology and growth propensities. To address the question about the nature of the observed relative growth propensities a set of interface surfaces was generated corresponding to the six initial interface configurations at the three temperatures tested in this work (see Fig. 5). The surfaces were generated using a three-dimensional version of the interface detection method described in ref. 3, so that instead of a Z-profile of the molecular density a three-dimensional map of the molecular density was used for surface detection and the Fourier transforms were obtained along the X, Y, and Z-directions (more details on the surface generation method will be provided in a forthcoming publication[23]). The molecular densities for the surface extraction were collected during the first 10 ps of simulations in all the runs and then averaged over all 200 isoconfigurational runs to produce a single isoconfigurational molecular density corresponding to the initial 10 ps. The isoconfigurational surfaces found from these average molecular density data, therefore, represent the initial isoconfigurational

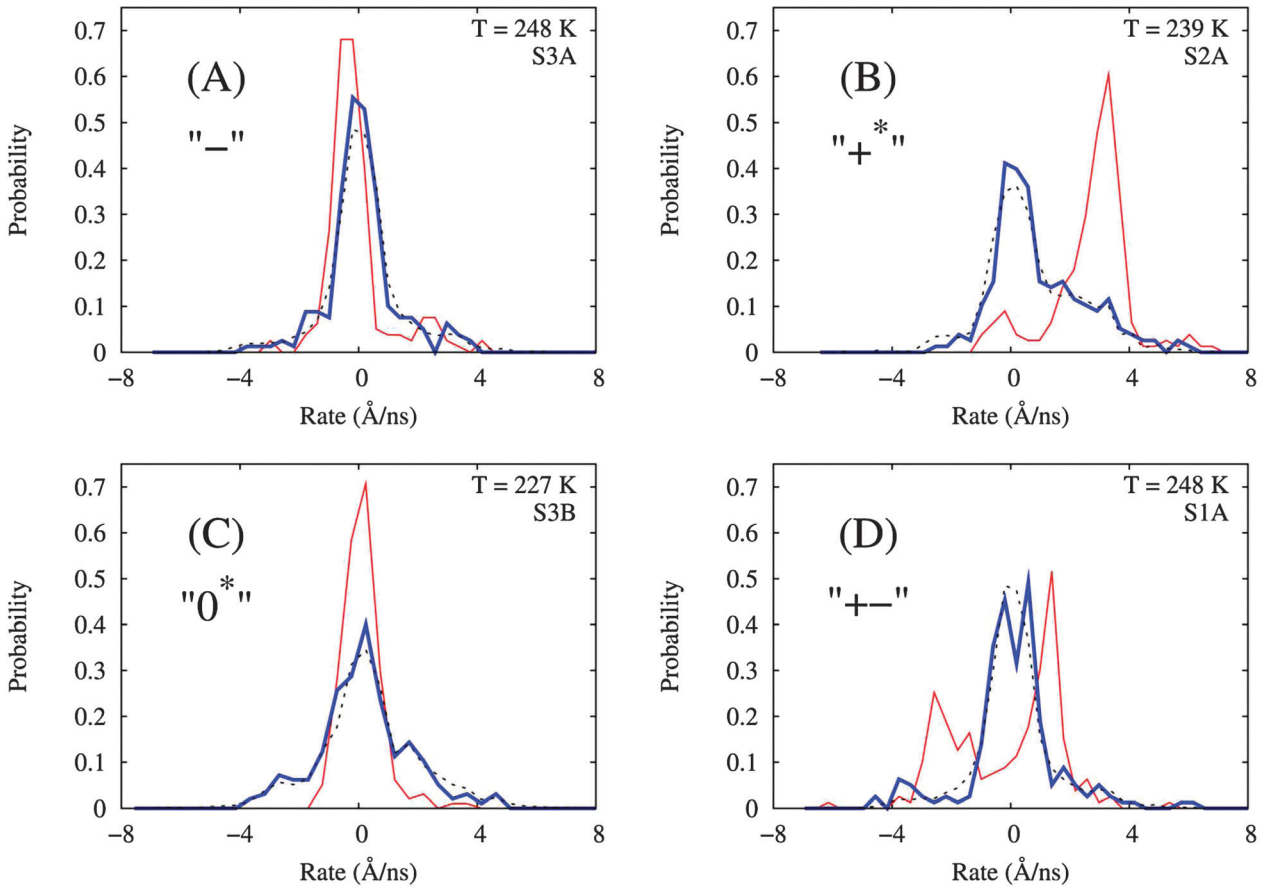

Fig. 4 Examples of probability distributions of 200 isoconfigurational ice growth rates (based on 1 ns time windows) demonstrating different kinds of relative growth propensity: (A), slower than average, (B), much faster than average, (C), similar mean but more narrow distribution, (D), similar mean but wider distribution. The rate distributions are shown at the beginning (thin lines) and at the end (thick lines) of the simulation. For comparison, the dashed lines show the average rate distribution "natural" to the specific temperature, taken as the distributions averaged over six isoconfigurational runs (thick lines in Fig. 3). The temperature, system, and interface for a specific isoconfigurational simulation are indicated in the top right corner of the plots. The notation used for a specific propensity is also shown in each graph in quote marks.

Table 3 Relative growth propensities of the six initial interfacial configurations at the three temperatures using 1 ns rate distributions. The following notation is used: "+", faster than average, "–", slower than average, "0", similar to average, "0*", similar to average but more narrow distribution, "+–", similar to average but wider distribution; the starred signs "+*" and "–*" indicate strong behaviour. Note that configurations with the same labeling at different temperatures are different

T	S1A	S1B	S2A	S2B	S3A	S3B
227	+*	–	0	–*	+	0*
239	+	0*	+*	0	+	0
248	+–	+	0*	+	–	–*

surface topology responsible for the relative growth propensities observed in this work.

Fig. 5 shows the four isoconfigurational interface surfaces corresponding to the rate distributions shown in Fig. 4. The case of a mild negative relative growth propensity is shown in Fig. 4(A). After examining the interface surface shown in Fig. 5(A) it becomes clear that the initial position of the planar interface is shifted to the liquid phase due to the presence of two crystal islands on the surface. These islands, however, are not sufficiently stable to complete a new ice layer and melt with high probability during the first 1 ns of the simulations, causing the rate distribution shown in Fig. 4(A) and the negative growth propensity.

Fig. 5(C) demonstrates an interface surface with a neutral growth propensity from Fig. 4(C) with the interface being more stable than expected at this temperature. The surface in Fig. 5(C) features a number of small ice islands and small pits in the ice crystal at the same time. Apparently, none of these islands and pits are sufficiently large to cause neither formation of a new ice layer nor melting of the top layer and will disappear with high probability in the next 1 ns. Such a behaviour will maintain the current position of the planar interface and explains the observed rate distribution.

While the cases shown in Fig. 5(A) and (C) are relatively simple so that the growth behaviour can be reasonably linked to the surface topology after simple visual analysis, the growth patterns shown in Fig. 4(B) and (D) and interface surfaces in Fig. 5(B) and (D) are significantly more complex. The interface shown in Fig. 5(B) has strong propensity to grow (Fig. 4(B)). Visual examination of its topology reveals that it is a complex three-dimensional surface involving 4 layers of ice; better understanding of such a complex case requires a more advanced analysis technique, which was not available at the time of writing.

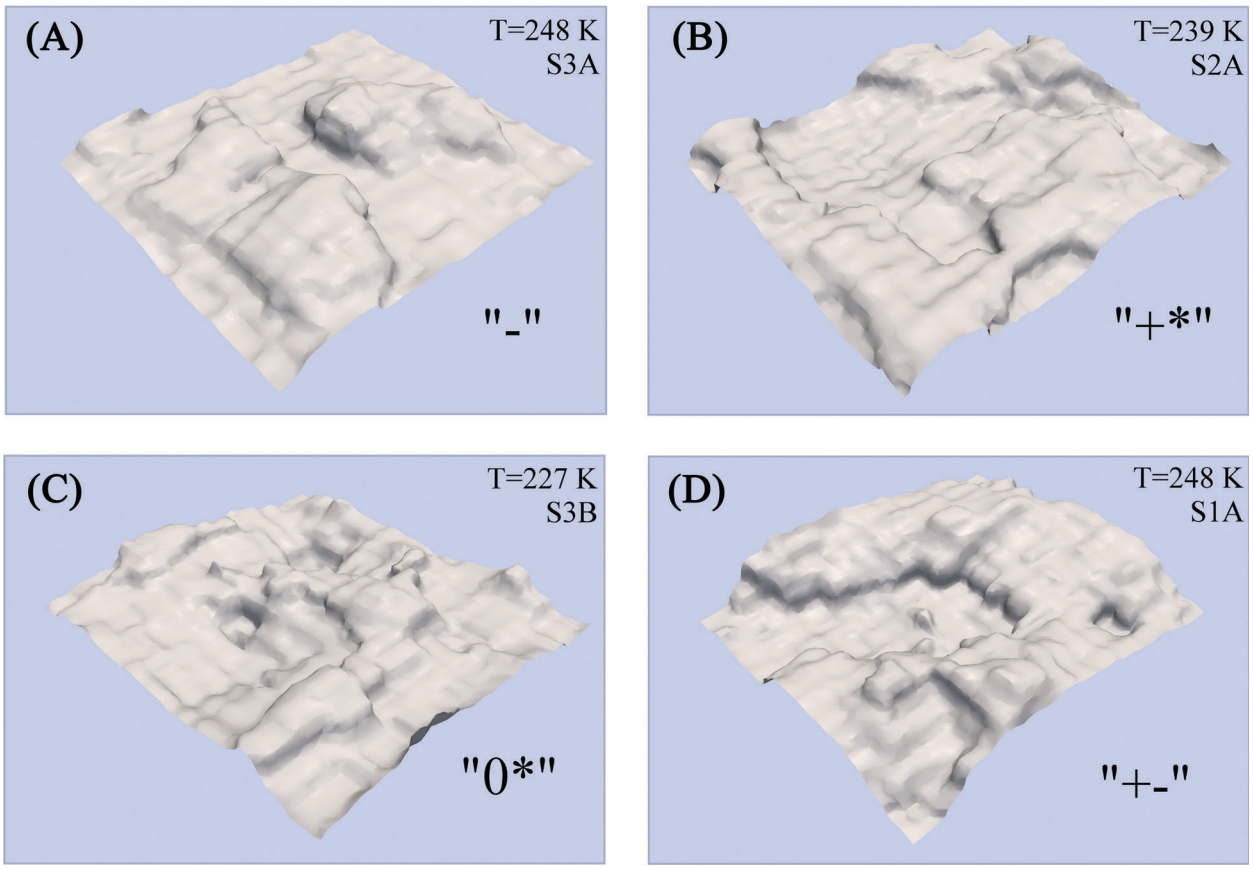

Fig. 5 Initial interface surfaces based on a structural order parameter averaged over the first 10 ps of simulation and over 200 isoconfigurational trajectories. The four interfaces corresponding to the rate distributions shown in Fig. 4 are shown: (A) S3A at 248 K, (B) S2A at 239 K, (C) S3B at 227 K, (D) S1A at 248 K. The ice phase is below the surface and the liquid water is above the surface. The surface dimensions are approximately 27×31 Å^2 and the thickness of one ice layer is about 3.7 Å. The notation used for a specific propensity is also shown in each graph in quote marks.

A similarly complex case is shown in Fig. 4(D) and 5(D), where a transition state of ice layer formation is demonstrated. One can see that the size of the ice island and the defect are comparable, but more analysis is required for deeper understanding of the properties of such a configuration. The interface surface plots for the other isoconfigurational simulations performed in this work are given in Fig. S4–S6, ESI†;[20] the surfaces correspond to the rate distributions shown in Fig. S1–S3 of ESI.†

5 Conclusions

By performing a number of isoconfigurational molecular dynamics simulations of ice growth at the basal face of the hexagonal ice I_h at different temperatures below the melting point it has been shown that a specific structure at a growing ice–water interface is able to affect the growth process at the time scale of 1–2 ns. This structural effect can be characterized in terms of relative growth propensities. After 2 ns this structural effect disappears and simulations become independent as the structures at the interfaces in different isoconfigurational runs diverge. It has been shown that after 2 ns the structural variation within the initially isoconfigurational set of simulations represents the typical structural variation at a specific temperature.

By averaging 1200 ice growth rates from 2 ns independent segments of simulations at three different temperatures new estimates for the growth rates of TIP4P-2005 ice have been determined to be 0.46 ± 0.06, 0.71 ± 0.06, and 0.18 ± 0.05 Å ns^{-1} for 227, 239, and 248 K, respectively. The new estimates are the most accurate to date. This method of finding growth rates is more efficient than the usual practice of finding the rates from long simulations and is effectively a steady-state one, as the system does not change much during a single short simulation.

The probability distributions of the isoconfigurational growth rates have been found to provide valuable insight into the nature of relative growth propensities for specific configurations. On the ground of the differences in the shape between isoconfigurational rate distributions and the rate distribution typical of the specific temperature five different kinds of relative growth propensities have been identified. The initial interfacial configurations employed in this work have been assigned using the proposed classification and possible mechanisms of propensity realization have been suggested for selected cases. The relative growth propensity specific to a surface configuration reflects a space–time variation in local thermodynamic properties at the interface arising from fluctuations. Such local changes in interface properties influence the probability of events associated with growth (melting) and can result in growth patterns different from expected average behaviour.

The interface configurations were obtained as isoconfigurational three-dimensional dividing surfaces using a structural order parameter. These configurations were compared with corresponding rate distributions and the observed relative growth propensities were explained from the structural point of view in some cases. A need for developing new methods of topological analysis of interface surfaces was clearly demonstrated for cases when a complex interface configuration results in an unusual growth behaviour.

We conclude that the results reported in this paper provide new important insight into mechanisms of crystal growth as well as other self-assembling processes. The structural effect on ordering propensities must be a universal behaviour, and expected to be seen in other similar problems such as protein folding, for example. The drawback of this isoconfigurational approach is that it is difficult to identify and visualize the actual structure pertinent to the simulation as the analysis is done on many diverging molecular dynamics trajectories. The work to address this shortcoming is currently underway.

Acknowledgements

We are grateful for financial support from the Natural Science and Engineering Research Council of Canada, the Canada Foundation for Innovation, and the University of Calgary.

References

1 M. S. G. Rasul, *Computer simulaiton studies of heterogeneous crystal growth*, PhD thesis, Dalhousie University, Halifax, Nova Scotia, 2005.
2 H. Nada, J. P. van der Eerden and Y. Furukawa, A clear observation of crystal growth of ice from water in a molecular dynamics simulation with a six-site potential model of H_2O, *J. Cryst. Growth*, 2004, **266**, 297–302.
3 D. Rozmanov and P. G. Kusalik, Temperature dependence of crystal growth of hexagonal ice (I_h), *Phys. Chem. Chem. Phys.*, 2011, **13**, 15501–15511.
4 D. Rozmanov and P. G. Kusalik, Crystal growth rates of ice from molecular dynamics simulations, *to be published*, 2012.
5 A. Widmer-Cooper, P. Harrowell and H. Fynewever, How reproducible are dynamic heterogeneities in a supercooled liquid? *Phys. Rev. Lett.*, 2004, **93**(13), 135701.
6 A. Widmer-Cooper and P. Harrowell, On the relationship between structure and dynamics in a supercooled liquid, *J. Phys.: Condens. Matter*, 2005, **17**, S4025–S4034.
7 G. S. Matharoo, M. S. G. Razul and P. H. Poole, Structural and dynamical heterogeneity in a glass-forming liquids, *Phys. Rev. E: Stat. Phys., Plasmas, Fluids, Relat. Interdiscip. Top.*, 2006, **74**, 050502–050504.
8 J. L. F. Abascal and C. Vega, A general purpose model for the condensed phases of water: TIP4P/2005, *J. Chem. Phys.*, 2005, **123**, 234505-1–12.
9 R. G. Fernandez, J. L. F. Abascal and C. Vega, The melting point of ice I_h for common water models calculated from direct coexistence of the solid-liquid interface, *J. Chem. Phys.*, 2006, **124**, 144506.
10 V. F. Petrenko and R. W. Whitworth, *Physics of Ice*, University Press, Oxford, 2002.
11 J. D. Bernal and R. H. Fowler, A Theory of Water and Ionic Solutions, with Particular Reference to Hydrogen and Hydroxyl Ions, *J. Chem. Phys.*, 1933, **1**(8), 515–548.
12 U. Essmann, L. Perera, M. L. Berkowitz, T. Darden, H. Lee and L. G. Pedersen, A smooth particle mesh Ewald method, *J. Chem. Phys.*, 1995, **103**(19), 8577–8593.
13 W. C. Swope, H. C. Andersen, P. H. Berens and K. R. Wilson, Computer simulation method for the caluculation of equilibrium constants for the formation of physical clusters of molecules: Application to small water cluseters, *J. Chem. Phys.*, 1982, **76**(1), 637–649.
14 D. Rozmanov and P. G. Kusalik, Robust rotational-velocity-Verlet integration methods, *Phys. Rev. E: Stat. Phys., Plasmas, Fluids, Relat. Interdiscip. Top.*, 2010, **81**, 056706.
15 G. J. Martina, M. L. Klein and M. Tuckerman, Nosé-Hoover chains: The canonical ensemble *via* continuous dynamics, *J. Chem. Phys.*, 1992, **97**(4), 2635–2643.
16 S. Jang and G. A. Voth, Simple reversible molecular dynamics alhorithms for Nosé-Hoover chain dynamics, *J. Chem. Phys.*, 1997, **107**(22), 9514–9526.
17 H. J. C. Berendsen, J. P. M. Postma, W. F. van Gunsteren, A. DiNola and J. R. Haak, Molecular dynamics with coupling to an external bath, *J. Chem. Phys.*, 1984, **81**(8), 3684–3690.
18 H. Nada and Y. Furukawa, Anisotropic growth kinetics of ice crystals from water studied by molecular dynamics simulation, *J. Cryst. Growth*, 1996, **169**, 587–597.
19 H. Nada and Y. Furukawa, Anisotropy in Molecular-Scaled Growth Kinetics of Ice–Water Interfaces, *J. Phys. Chem. B*, 1997, **101**, 6163–6166.
20 D. Rozmanov and P. G. Kusalik, *Phys. Chem. Chem. Phys.*, 2012, DOI: 10.1039/c2cp41073g. See ESI†.
21 J. Vatamanu and P. G. Kusalik, Microfaceting and its implication in the nonrandom stacking in fcc crystals, *Phys. Rev. B: Condens. Matter Mater. Phys.*, 2007, **76**, 035431–035436.
22 J. Vatamanu and P. G. Kusalik, Heterogeneous crystal growth of methane hydrate on its sii [001] crystallographic face, *J. Phys. Chem. B*, 2008, **112**, 2399–2404.
23 D. Rozmanov and P. G. Kusalik, *to be published.*

